Space object detecting ability improvement method based on optimal principle*

GAO Yang (高扬)[1,2]** **and ZHAO Jin-yu** (赵金宇)[1]

1. Changchun Institute of Optics, Fine Mechanics and Physics, Chinese Academy of Sciences, Changchun 130033, China

2. University of Chinese Academy of Science, Beijing 100039, China

(Received 26 December 2018; Revised 6 March 2019)

©Tianjin University of Technology and Springer-Verlag GmbH Germany, part of Springer Nature 2019

In view of the increasing threat of massive satellites and orbital debris to space launch missions, an optimization method of ground-based optoelectronics surveillance system is proposed. Passive optical system can monitor space target at a cost-effective way. This paper analyzes the detection ability of telescope and the optical reflection characteristics of high orbital objects, combined with the motion characteristics and observation conditions of high orbital debris, and thus analyzes the detection and recognition ability of space targets by the ground optoelectronics system. In order to solve the problem of faint targets detection, the optimization principle of star image with low signal-to-noise ratio (*SNR*) is demonstrated. Compared with the traditional frame difference method, the spatial targets with *SNR* greater than 3.10 can be identified without changing the aperture of observation equipment.

Document code: A **Article ID:** 1673-1905(2019)06-0459-4

DOI https://doi.org/10.1007/s11801-019-8204-4

The newest released status by European space agency (ESA) shows that there are more than 750 000 pieces of debris (larger than 1 cm) in earth orbit[1]. The rapidly expanding population of space objects has brought great threat to the sustainable development of space activities such as space craft launching and space station[2,3]. Space surveillance plays a critical role in pre-launch alert and collision avoidance[4]. According to orbit height, space objects can be classified as low earth orbit (LEO) and geosynchronous orbit (GEO). Detecting capability of radar is inversely proportional to biquadrate of distance, optoelectronic system detecting capability is inversely proportional to quadrate of distance, therefore optoelectronic surveillance is more suitable for high orbit debris[5].

With the support of defense advanced research project agency of the US, in 2011 a ground-based telescope capable of monitoring 21 600 objects - space surveillance telescope (SST) was deposed in white sands missile range (WSMR)[6-8]. Of all earth orbit objects, 23 000 are regularly tracked by the US space surveillance network and maintained in their catalogue including objects larger than about 5—10 cm in LEO and 30 cm to 1 m at GEO altitudes among which only a small fraction (about 1 200) are operational satellites[9-11].

The object detection ability of the optoelectronic system is affected by telescope structure, observation location, atmosphere and process method of the image detected[12]. Common object detection methods, such as difference frame method, local adaptive threshold segmentation and so on, requires a better than 6 signal-to-noise ratio (*SNR*)[13-15]. To improve the detection ability of telescopes under the same caliber, this paper proposes an optimization principle of passive optical system in high orbit debris monitoring. Based on this principle, a new faint targets detection method is presented.

The efficacy of ground-based optoelectronic surveillance system can be estimated by analyzing telescope detection ability and optical properties of orbit objects.

CCD detector is the vital section in a telescope detection system which collects photons then turns them into electrons. CCD pixel number and pixel size, quantum efficiency, noise, charge transfer efficiency is the main concerned parameters when CCD detector is used in space object detection mission. In the case of a given observation station, a telescope's optical system structure and a given CCD detector, the detection ability of the telescope can be estimated.

The number of photons received by a telescope is

$$N_{\mathrm{obj}} = C \times \frac{\pi}{4} \times D^2 \times \tau \times \gamma \times t \times QE \,, \tag{1}$$

where C represents the magnitude M photon emission in sun light spectrum within 450—900 nm, C=3.44×10^6×$10^{-0.4M}$, D is the telescope aperture, τ is atmospheric

* This work has been supported by the Third Phase of Innovative Engineering Projects of Changchun Institute of Optics, Fine Mechanics and Physics, Chinese Academy of Sciences (No.065X32CN60).

** E-mail:gyslashgy@163.com

transmittance, γ is efficiency of optical system, t is target exposure time, and QE is CCD quantum efficiency.

Target exposure time t refers to the target in a pixel on the residence time:

$$t=\frac{(\sqrt{K}+B-1)\times A}{v}\ , \tag{2}$$

where v is the velocity of the target, A is each pixel size, K is the number of pixels of the target, and B is the number of pixels that CCD reads in BIN.

The optical properties of space objects can vary from shape, material orientation and position of observer. Assuming the object is spherical with diameter d and reflectance R, the visual magnitude of the object is:

$$M_{\text{obj}}=-26.74-2.5\log\frac{d^2\times R\times p(\omega)}{S^2}\ , \tag{3}$$

where S represents the distance from observer to object, ω is solar phase angle, $p(\omega)$ is solar phase angle function, and −26.74 is visual magnitude of sun.

A zero magnitude source provides 1.78×10^{-8} W/m^2 over typical spectral at CCD sensor. The irradiance photon number per square meter of second can be calculated as:

$$E_{\text{obj}}=\frac{\lambda\times1.78\times10^{-8}}{h\times c\times10^{-8}\times2.512^{M_{\text{obj}}}}\ , \tag{4}$$

where λ is wavelength, h is Planck constant, and c is the speed of light.

For space object, primary noise of ground-based optoelectronic system includes skylight background noise, CCD dark current and readout noise. When the exposure time is shorter, the influence of the CCD dark current is quite small. The read-out noise is mainly derived from the first order field effect transistor amplifier, which is proportional to the square root of the frequency band width of the system.

The number of light photons per pixel is:

$$N_{\text{sky}}=C'\times\frac{\pi}{4}\times D^2\times\tau\times\gamma\times t_{\text{CCD}}\times A^2\times QE\ , \tag{5}$$

where C' represents background skylight photon emission which is determinated by tg Skylight, $C'=3.44\times10^6\times10^{-0.4tg}$.

$$t_{tg}=\frac{(\sqrt{K}+B)\times A}{v}\ . \tag{6}$$

Detectable SNR is:

$$\frac{S}{N}=\frac{N_{\text{obj}}\times\beta}{\sqrt{N_{\text{obj}}\times\beta+N_{\text{sky}}\times\beta+N_{\text{dark}}\times t+\sigma_{\text{read}}^2}}\ , \tag{7}$$

where β is the target starlight dispersion factor, it is generally the inverse of the number of astrological pixels, N_{dark} is the CCD dark current, and σ_{read} is the CCD readout noise of one pixel.

Although the geostationary orbit satellite stays relatively stationary with the earth, the objects in the GEO region do not remain in a quiescence position. Due to the perturbation of the sun and the moon, the GEO orbit objects inclination angle increases, resulting in north-south velocity component. Sub-stellar point change of typical large angle GEO object is shown in Fig.1.

Meanwhile, different object height on the GEO array will produce east-west velocity component. The objects below the GEO orbit region will have higher orbital speed, thus produce an eastward velocity component relative to static GEO position. Similarly, the target above the GEO orbit region will produce westward velocity components. The north-south velocity component caused by the inclination angle reaches maximum when the GEO objects reach 0 declination. The north-south speed component equals 0 when the object is at north-south rotation point. The visual velocity is a function of height and inclination. The visual velocity change curve of the GEO object is shown in Fig.2.

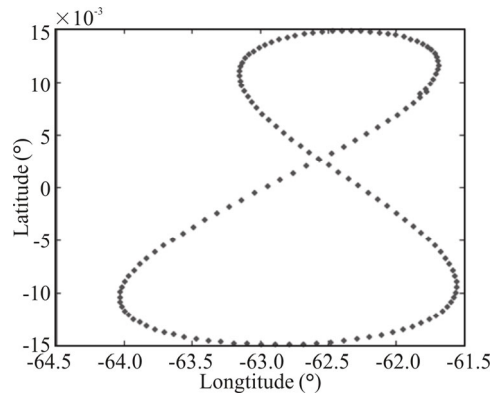

Fig.1 Sub-stellar point change of typical target

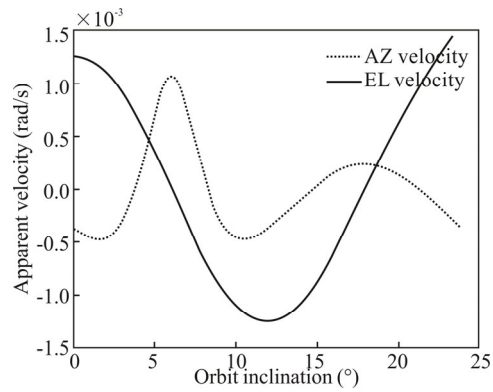

Fig. 2 Visual velocity change curve

The minimum recognizable high orbit debris SNR can be calculated. Tab.1 shows object SNR in different magnitudes and velocities, and the integrate time is adjusted to object velocity.

The ground-based telescope can obtain the location and brightness information of the orbit object by searching and tracking it. Due to the influence of background skylight, moonlight, star and field of view vignet, the $SNRs$ of different objects are different in the same frame. When CCD captured images processed by the traditional difference frame method or local adaptive threshold segmentation method, SNR should be better than 6 to recognize orbit objects from

background stars. In order to effectively detect space objects at a lower *SNR* and enhance the detection ability of telescopes under the same aperture, a new method based on optimization principle is proposed in this paper.

Tab.1 Calculated object *SNR* results

Object magnitude	Object velocity	Exposure time	CCD integrate time	Object *SNR*
11.4	0.1	50.8	68	5.20
11.6	0.1	50.8	68	4.41
10.9	0.2	25.4	34	5.07
11.1	0.2	25.4	34	4.32
10.5	0.3	16.9	23	5.31
10.7	0.3	16.9	23	4.53
10.3	0.4	12.7	17	5.11
10.5	0.4	12.7	17	4.37
10.0	0.5	10.2	14	5.48
10.2	0.5	10.2	14	4.70

A following optimization problem is constructed to obtain a superimposed image with only targets and random noise residual:

$$\arg\min Rank(\boldsymbol{A})+\|\boldsymbol{T}\|_0+\|\boldsymbol{\varepsilon}\|_2 \ , s.t.\ \boldsymbol{A}+\boldsymbol{T}+\boldsymbol{\varepsilon}=\boldsymbol{D} \ , \quad (8)$$

where matrix $\boldsymbol{D}$ represents the original image data. Matrix $\boldsymbol{A}$ represents the image background data including stars, matrix $\boldsymbol{A}$ is a low rank matrix, then the optimization objective function contains a minimization problem of $Rank(\boldsymbol{A})$, $Rank(\boldsymbol{A})$ is the rank of matrix $\boldsymbol{A}$. Matrix $\boldsymbol{T}$ represents the target matrix, the number of pixels of the target is quite small relative to the stars and the background, so $\boldsymbol{T}$ is a sparse matrix. Zero norm means the number of nonzero elements in matrix, then $\|\boldsymbol{T}\|_0$ is the number of targets, the optimization objective function contains a minimization problem of $\|\boldsymbol{T}\|_0$. Matrix $\boldsymbol{\varepsilon}$ represents noise, the optimization objective function contains a minimization problem of $\|\boldsymbol{\varepsilon}\|_0$. Image constraint condition is matrix $\boldsymbol{D}$, equals to the sum of matrix $\boldsymbol{A}$, matrix $\boldsymbol{\varepsilon}$ and matrix $\boldsymbol{T}$.

However, $Rank(\boldsymbol{A})$ is a non-convex and non-smooth function, which is difficult to be optimized as an objective function. $\|\boldsymbol{A}\|_*$ is the nuclear norm of matrix $\boldsymbol{A}$, it's the sum of singular values of matrix $\boldsymbol{A}$. $\|\boldsymbol{A}\|_*$ is the most compact convex envelope of $Rank(\boldsymbol{A})$, it's used to replace $Rank(\boldsymbol{A})$. Similarly, the optimization problem of the objective function $\|\boldsymbol{T}\|_0$ is a non-deterministic polynomial (NP-hard) problem commonly used $\|\boldsymbol{T}\|_1$ to replace it. Therefore, the optimization problem aforementioned is transformed to:

$$\arg\min\|\boldsymbol{A}\|_*+\lambda\|\boldsymbol{T}\|_1+\frac{\mu}{2}\|\boldsymbol{D}-\boldsymbol{A}-\boldsymbol{T}\|_2^2 \ , \quad (9)$$

where λ and μ are sensitivity coefficients in Lagrange multiplier. Use the Lagrange multiplier method to accelerate the aforementioned problem:

$$L=\|\boldsymbol{A}\|_*+\lambda\|\boldsymbol{T}\|_1+\langle Y,\boldsymbol{D}-\boldsymbol{A}-\boldsymbol{T}\rangle+\frac{\mu}{2}\|\boldsymbol{D}-\boldsymbol{A}-\boldsymbol{T}\|_2^2 \ . \quad (10)$$

Through the above mathematical process, we get the matrix $\boldsymbol{T}$, which is an image eliminate of stars, background and noise. It still contains noise residuals, which is caused by the optimization solving process, but generally the object *SNR* will be effectively enhanced by the optimization process. Fig.3 shows (a) an original star image processed by optimization method, resulting in (b) the solution image. The *SNR* of the target in the original image is 3.09, and the *SNR* of the target image is 4.63, which shows that the target *SNR* is significantly improved.

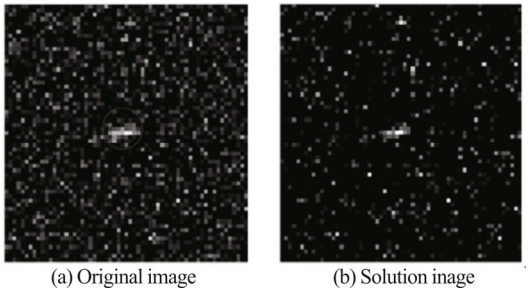

(a) Original image (b) Solution inage

Fig.3 Comparison between solution image and original image (target detail)

The objects recognition results using optimization method are shown in Fig.4. Frame difference method can recognize 6 targets, optimization identification method can recognize 7 targets, and all recognized results were none false alert targets. Frame difference method fails to recognize the one at the right edge of image whose *SNR* is 3.09. The optimization method improves *SNR* of the above target to 4.63 by differentiate processing the *SNR* between the foreground and the background, and extracts the target region. It can be seen that the detection ability of the optical telescope is improved without change the aperture of telescope and the recognition rate of space targets is higher.

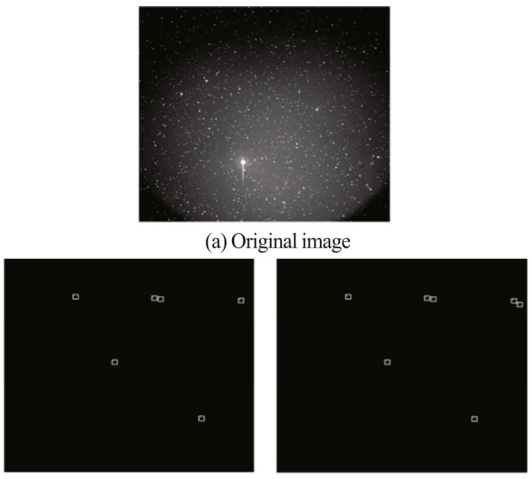

(a) Original image

(b) Image difference frame method (c) Optimal identification method

Fig.4 Recognition result comparison between optimization method and image frame difference method

In this paper, an object recognition method based on optimization principle is proposed to recognize GEO objects from ground-based optoelectronic detected images. By constructing the optimization problem under constraint conditions, the method can obtain solution image with higher target *SNR* and improve the recognition rate of the space objects out of background noise and stars. The experimental results show that the objects *SNR* is greatly improved and it can be identified after optimization processing. In addition, the optimal design elements of ground-based optoelectronic surveillance are expounded from the perspectives of telescope detection capability, space debris optical characteristics, motion characteristics which may provide references for the design of ground-based optoelectronic surveillance devices for GEO objects.

References

[1] Luo Hao, Mao Yin-dun, Yu Yong and Tang Zheng-hong, Opto-Electronic Engineering **44**, 418 (2017). (in Chinese)

[2] Wang Xue-yao, Spacecraft Engineering **27**, 86 (2018). (in Chinese)

[3] Wang Min, Automatic Recognition of Space Targets in Complex Background, Changchun Institute Optics, Fine Mechanics and Physics, Chinese Academy of Science, 2017. (in Chinese)

[4] T. Flohrer, T. Schildknecht and R. Musci, Advances in Space Research **02**, 1010 (2008).

[5] Li Bin, Researches on Key Technologies of Fast and Accurate Orbit Determination and Prediction of Space Debris, Wuhan University, 2017. (in Chinese)

[6] S. H. Craig and B. Greene, The EOS Space Debris Tracking System, The Advanced Maui Optical and Space Surveillance Technologies Conference, 2006.

[7] Tan Ji-bo, Huang Jian-yu, Wang Kun-peng and Wu Wen-tang, Acta Photonica Sinica **46**, 96 (2017). (in Chinese)

[8] J. Stupl, N. Faber, C. Foster, F. Yang and B. Nelson, Light Force Photon-pressure Collision Avoidance: Updated Efficiency Analysis Utilizing a Highly Parallel Simulation Approach, AMOS: Advanced Maui Optical and Space Surveillance Conference, 2014.

[9] T. Flohrer, T. Schildknecht, R. Musci and E. Stoveken, Advances in Space Research **03**, 1226 (2005).

[10] James R. Shell, Optimizing Orbital Debris Monitoring with Optical Telescopes, Advanced Maui Optical & Space Surveillance Technologies Conference, 2010.

[11] Pascal Richard, Simulation of Telescope Detectivity for GEO Survey and Tracking, Proceedings of the Advanced Maui Optical and Space Surveillance Technologies Conference, 2014.

[12] G. Kirchner, F. Koidl, F. Friederich, I. Buske and U. Volker, Advances in Space Research **51**, 21 (2013).

[13] P. Dao，R. Rast, W. Schlaegel, V. Schmid, S. Gregory and A. Dentamaro, Track-before-detect Algorithm for Faint Moving Objects Based on Random Sampling and Consensus, In Proceedings of the 2014 Advanced Maui Optical and Space Surveillance Technologies Conference, 2014.

[14] M. Uetsuhara and N. Ikoma, Faint Debris Detection by Particle Based Track-before-detect Method, In Proceedings of the 2014 Advanced Maui Optical and Space Surveillance Technologies Conference, 2014.

[15] W Krag, Visible Magnitude of Typical Satellites in Synchronous Orbits, Massachusetts: Massachusetts Institute of Technology, 1974.